



HAL
open science

Aging dynamics in Laponite dispersions at various salt concentrations

Barbara Ruzicka, Laura Zulian, Giancarlo Ruocco

► **To cite this version:**

Barbara Ruzicka, Laura Zulian, Giancarlo Ruocco. Aging dynamics in Laponite dispersions at various salt concentrations. *Philosophical Magazine*, 2007, 87 (3-5), pp.449-458. 10.1080/14786430600962732 . hal-00513767

HAL Id: hal-00513767

<https://hal.science/hal-00513767>

Submitted on 1 Sep 2010

HAL is a multi-disciplinary open access archive for the deposit and dissemination of scientific research documents, whether they are published or not. The documents may come from teaching and research institutions in France or abroad, or from public or private research centers.

L'archive ouverte pluridisciplinaire **HAL**, est destinée au dépôt et à la diffusion de documents scientifiques de niveau recherche, publiés ou non, émanant des établissements d'enseignement et de recherche français ou étrangers, des laboratoires publics ou privés.



Aging dynamics in Laponite dispersions at various salt concentrations

Journal:	<i>Philosophical Magazine & Philosophical Magazine Letters</i>
Manuscript ID:	TPHM-06-May-0171.R2
Journal Selection:	Philosophical Magazine
Date Submitted by the Author:	05-Aug-2006
Complete List of Authors:	Ruzicka, Barbara; Universita', Physics Zulian, Laura; Universita' di Perugia, Dip. di Fisica Ruocco, Giancarlo; Universita' "La sapienza", Dip. di fisica
Keywords:	colloids, phase diagrams, sol-gel
Keywords (user supplied):	light scattering



Ageing dynamics in Laponite dispersions at various salt concentrationsB.Ruzicka^{1,2,*}, L. Zulian^{2,3}, G. Ruocco^{1,2}¹*Dip. Fisica, Università di Roma "La Sapienza", P.le A. Moro 2, I-00185 Roma*²*CNR-INFM, CRS SOFT Università Roma "La Sapienza", P.le A. Moro 2, I-00185 Roma*³*Dip. Fisica Università di Perugia, Via A. Pascoli, I-06123 Perugia, Italy*

For Peer Review Only

*Corresponding author. Email: barbara.ruzicka@phys.uniroma1.it

Abstract

The ageing dynamics of a charged colloidal system, Laponite suspensions in water, has been investigated by a photon correlation technique. The samples have a very wide range of clay concentrations ($C_w = 0.3-3.1$ % in weight) and four different NaCl salt concentrations ($C_s = 1 \times 10^{-4}$ M; 1×10^{-3} M; 2×10^{-3} M; 5×10^{-3} M) and have been studied in a novel way to investigate the phase diagram, which has been subject of discussion in recent literature. A clear picture of the Laponite phase diagram has been obtained. The measurements show the existence of two different dynamical routes to reach a final arrested state and the presence of a transition line between them in the C_w - C_s plane.

§1. Introduction

In recent years, Laponite dispersions in water have been widely studied on account of the peculiarity of their phase diagram, originating from a competition between the short-range attractive and long-range repulsive interactions, and the ability of varying the clay concentration and/or ionic strength of the dispersions [1-7, 9-11, 13-16]. Moreover, despite intensive research on the subject, only very recently it has been observed that this system can form an arrested phase also at very low clay concentrations. The discovery of this arrested phase at weight concentration as low as $C_w = 0.3$ % [17] gives further interest to the study of this charged colloidal system. As in the usually studied part of the phase diagram (at $C_w = 3$ % and $C_s = 1 \times 10^{-4}$ M) [1-3, 5, 6], ageing dynamics of Laponite, quenched out of equilibrium by shearing the system, has also been observed in the region of very low clay concentrations. In this paper, samples with a very wide range of clay and salt concentrations, have been studied in detail and the ageing behaviour identified and analysed for all the investigated concentrations. An arrested state has been identified for all the samples and a phase diagram with two different arrested phases, at "low" and "high" clay concentrations, is proposed.

§2. Experimental details

Laponite in water is a colloidal dispersion of charged disk-like particles. The clay powder is composed of single crystals with a three-layer structure. The central one contains magnesium and

1
2
3 lithium atoms bonded with oxygen and OH groups to form an octahedral structure. This layer is
4
5 sandwiched within two tetrahedral structures of silicon with sodium atoms that are exposed on the
6
7 surface of the platelets [8]. When this kind of chemical architecture is dispersed in water, Na ions
8
9 are released on the surface by ionization, forming a net negative charge of some hundreds of
10
11 elementary charges. In addition, owing to protonation of the OH groups disposed on the rim of the
12
13 plate, a weak positive charge also appears. Therefore both attractive and repulsive interactions are
14
15 present in this charged colloidal system.
16
17
18

19
20 For the case of salt-free water ($C_s = 1 \times 10^{-4}$ M) the samples are prepared by mixing Laponite
21
22 powder with deionized water (18 m Ω) in the weighted proportions. Otherwise Laponite is dispersed
23
24 in a solution of deionized water and NaCl salt with concentrations: $C_s = 1 \times 10^{-3}$ M, 2×10^{-3} M, and
25
26 5×10^{-3} M. The dispersions are vigorously stirred until the solutions become clear. For
27
28 reproducibility reasons this time is kept to 30 minutes for all samples. Just after the stirring, the
29
30 dispersion is filtered through a Millipore 0.45 μ m pore size filters and at this moment the initial
31
32 waiting time $t_w = 0$ is defined. The determination of the concentration of the samples is problematic
33
34 as the filtering procedure can alter the actual concentration if large clusters are present in the
35
36 suspension after the stirring phase. To minimize this effect, we prepared a large amount of
37
38 concentrated solution at each salt content, then we diluted this parent sample at the desired
39
40 concentrations. In this way the *relative* concentrations are well defined, even if the absolute value in
41
42 C_w can be affected by a systematic error, which we estimate to be in the range $\Delta C_w / C_w \cong 0.1$. The
43
44 whole procedure has been performed inside a glove box in a nitrogen atmosphere to avoid any
45
46 contact of the samples with atmospheric CO₂ which could cause a degradation or a dissolution of
47
48 Laponite crystals [12], [21]. No titration has been performed on Laponite samples, but a complete
49
50 study of it can be found in reference [21].
51
52
53
54
55
56
57

58 Dynamic light scattering measurements were performed. For none of the samples was a
59
60 significant multiple-scattering signal expected or revealed. Therefore an ALV-5000 logarithmic
correlator in combination with a standard optical set-up based on a He-Ne ($\lambda = 632.8$ nm) 10 mW

1
2
3 laser and a photomultiplier detector was used. The intensity correlation function was directly
4
5 obtained as $g_2(q; t) = \langle I(q; t)I(q; 0) \rangle / \langle I(q; 0) \rangle^2$, where q is the modulus of the scattering wave
6
7 vector defined as $q = (4\pi n/\lambda) \sin(\theta/2)$ ($\theta = 90^\circ$ in the present experiment). The acquisition time was 5
8
9 minutes for all the measurements.
10
11

12 § 3. Results and discussion

13
14
15
16
17 In Figure 1 the raw spectra obtained by photon correlation measurements are shown for two
18
19 samples, at "low" and "high" clay concentrations, respectively $C_w = 1.0\%$ (panel B) and $C_w = 2.5\%$,
20
21 (panel A) for a salt concentration of $C_s = 2 \times 10^{-3}$ M at the waiting times t_w reported in the figure.
22
23 The figure shows clearly that both samples are undergoing ageing, i.e. the correlation time increase
24
25 for an increase in the waiting time. The measured spectra show also that, for both samples, at the
26
27 longest reported ageing time, there is a transition towards an arrested phase as indicated by the
28
29 evolution of the autocorrelation spectra from a complete decay to zero to an incomplete decay to a
30
31 pseudo plateau (red curves in Fig. 1).
32
33

34
35 This is the clear signature that, after a time that depends on clay and salt concentrations (as shown
36
37 below), the samples undergo an ergodic to non-ergodic transition, representing a jump from the
38
39 liquid to an arrested phase, as already reported in references [3], [6] and [13]. Also a direct
40
41 inspection of the samples shows that the initial as-prepared liquid phase becomes a fully arrested
42
43 phase, whereby the sample supports its own weight if turned upside down. The same behaviour has
44
45 been observed for all the investigated samples, showing that for all the different clay and salt
46
47 concentrations an arrested phase can be found.
48
49
50

51
52 [Insert figure 1 about here]
53

54
55 The spectra decay with a two step behaviour, more visible at long waiting times, and furthermore
56
57 they can be described by two relaxation processes. From Fig. 1 one can observe that the ageing
58
59 evolution is different for the two series of samples: in fact for the series of samples at "low"
60
concentrations (panel B of the figure) the whole of the curve evolves with waiting time, while for

the series at "high" concentrations (panel A of the figure) the first decay seems to be fixed while the second one is more sensitive to the ageing time.

The two-step behaviour of all the measured autocorrelation curves can be described as the squared sum of two terms: the first fast decay, is obtained by a simple exponential term while the second slow decay, can be described by a stretched exponential term in the following way:

$$g_2(q,t) - 1 = b[a \exp(-t/\tau_1) + (1 - a) \exp(-(t/\tau_2)^\beta)]^2$$

Here b is the coherence factor, a and $(1 - a)$ are the weights of the two contributions τ_1 and τ_2 , which in turn are the fast and the slow correlation times, while β is the stretching parameter. The fit analysis has been performed successfully on all the spectra in the ergodic (liquid) phase, as can be seen from the full lines superimposed to the experimental points in Fig. 1. From this analysis all the parameters can be extracted with the error bars obtained by the fit analysis assuming a constant error on the experimental data. We will focus now our attention on the parameters of the slow decay - the stretched exponential term of the fit.

One can calculate a mean relaxation time τ_m of the relaxation time distribution of the stretched exponential term through the slow relaxation time τ_2 and the stretching exponent β , as described in reference. [19]:

$$\tau_m = \tau_2 \frac{1}{\beta} \Gamma\left(\frac{1}{\beta}\right) \quad (2)$$

where Γ is the Euler gamma function.

Another way to obtain a mean correlation time from a stretched exponential distribution is to calculate the mean value of the natural logarithm of the slow correlation time, which can be demonstrated to be given by:

$$\tau_{m2} = \tau_2 \exp\left(\gamma \left(1 - \frac{1}{\beta}\right)\right)$$

where γ is the Euler constant.

1
2
3 A comparison of τ_m , τ_{m2} and τ_2 is reported in Fig. 2 for a “low” concentration sample ($C_w =$
4 0.6 %, bottom panel) and a “high” concentration sample ($C_w = 2.5$ %, top panel) both at $C_s = 1 \times 10^{-3}$
5 M. The figure shows clearly that, both at low and at high clay concentrations, the general trend of
6 the three possible definitions of the correlation times is essentially the same. So the features found in
7 the following analysis and in our previous works [17-19] cannot be considered to arise simply from
8 our definition of the mean correlation time τ_m and can be extended to τ_2 and τ_{m2} .
9
10
11
12
13
14
15
16

17 [Insert figure 2 about here]
18

19 The mean correlation time τ_m and the stretching parameter β are linked through relation (2). The
20 behaviour of the mean correlation time τ_m as a function of the stretching parameter β for all the
21 studied clay and salt concentrations (indicated as circles in Fig. 6) is reported in Figure 3. From this
22 figure it is evident that for each salt concentration (decreasing from the top to the bottom of the
23 figure, from panel A to panel D) τ_m is always decreasing as β is increasing and that all the different
24 clay concentrations collapse on a single master curve. This suggests that a general trend for all the
25 clay concentrations at a fixed salt concentration can be found.
26
27
28
29
30
31
32
33
34
35

36 [Insert figure 3 about here]
37

38 Moreover if we plot τ_m with respect to β for different clay and different salt concentrations on the
39 same graph, in this case also all the curves collapse onto a single curve. This comparison is reported
40 in Figure 4 where one clay concentration for each salt concentration are plotted together without
41 any scale factor. The figure shows clearly that also for the four investigated salt concentrations the
42 curves superimpose.
43
44
45
46
47
48
49

50 [Insert figure 4 about here]
51

52 These comparisons indicate a strong correlation between the two parameters for all the investigated
53 samples and that a master curve for all the different salt and clay concentrations can be found.
54
55
56

57 The mean correlation time can be fitted by a phenomenological law that describes its
58 apparent divergence [17, 18]:
59
60

$$\tau_m = \tau_0 \exp (B t_w / (t_w^\infty - t_w))$$

The fit analysis well describes all the samples, both the "low" and the "high" clay concentrations. An indication of the quality of the fits can be seen by the full lines reported on the experimental points for the "low" (bottom panel, $C_w = 0.6 \%$) and the "high" (top panel, $C_w = 2.5 \%$) concentration samples at $C_s = 1 \times 10^{-3} \text{ M}$ reported as an example in the already discussed Figure 2. Different fits of the τ_m values at other clay and salt concentrations can be found in Fig. 3 of reference [19].

The data analysis permits us to obtain the two important parameters that describe the ageing process: the B parameter, which measures how fast τ_m approaches the divergence, and the t_w^∞ parameter, which indicates the waiting time at which the divergence occurs, i.e. the time at which the system is arrested. These two parameters have been fully discussed in reference [19]; here we limit ourselves to show their general trend in Figure 5. In this Figure the behaviour as a function of the ageing time for all the clay concentrations and for the four salt concentrations investigated, decreasing from the top to the bottom panel, are reported. This complete study has permitted differentiation of the ageing process in "low" and "high" concentration samples. In particular, with the measurements of salt-free water samples ($C_s = 10^{-4} \text{ M}$), we have found two different master curves: one for the "low" and the other for the "high" concentration samples - for more details, see [17-18]. Moreover from the study of other samples at higher salt concentrations we can now generalize our findings [19] to this part of the phase diagram and define "low" and "high" concentration samples as the ones at, respectively, "low" and "high" values of B. These two series of samples are distinguished in the figure by, respectively, open and full circles. Performing then a sigmoidal fit of the B parameter, reported as dashed lines in panel (A) of Fig. 5, we can also extract a mean value for each salt concentration that defines the point in between the two behaviours; these are indicated by stars in Fig. 6. Panel B of Fig. 5 shows that, for all the studied samples, there is a t_w^∞ at which the final state of all the studied samples is arrested. The arresting time depends on clay

1
2
3 and salt concentrations, decreasing for increasing clay and/or salt concentrations. Therefore the
4
5 ageing dynamics at both high clay and salt concentrations is too fast to be followed with the photon
6
7 correlation technique.
8
9

10 [Insert figure 5 about here]
11

12 In Figure 6 we report the phase diagram of Laponite suspensions as derived from our
13
14 measurements. All the investigated samples are reported in the graph as circles (open or full in
15
16 accordance with Fig. 5) and all are in a final arrested state. This new phase diagram is not trivial
17
18 because it rules out the previous assignation of the low free-concentration region as an isotropic
19
20 stable liquid phase [11], [20]. As already discussed, our new findings fully establish that also at low
21
22 clay concentrations, both in salt-free water [17-18] and in added salt water [19], an arrested phase
23
24 can be found. Moreover from the measured spectra (see the discussion about the general evolution
25
26 of the ageing curves) and, more quantitatively from the behaviour of the B parameter, a difference
27
28 in the ageing process for the "low" and "high" concentration samples has been found. The sigmoidal
29
30 fit and the stars points of Fig. 5 reported in Fig. 6 permit us to draw a line that separates two
31
32 different dynamical arresting processes: IG1 and IG2.
33
34
35
36
37

38 [Insert figure 6 about here]
39
40
41
42

43 § 4. Conclusions 44

45 From this study of Laponite suspensions in water with wide clay and salt concentrations, the
46
47 ageing process of this charged colloidal system has been investigated. The fundamental parameters
48
49 of the evolution towards the arrested state have been obtained and their behaviours have shown two
50
51 different dynamical ways to reach the final arrested state. A new gel or glass phase has been found
52
53 at clay concentrations as low as $C_w = 0.3 \%$, at several salt concentrations (IG1 region in Fig. 6).
54
55 The analysis has permitted to distinguish between two different arrested phases, IG1 and IG2 of
56
57 Fig. 6, and to draw a transition line between them in the Laponite phase diagram.
58
59
60

References

1
2
3
4
5
6
7
8
9
10
11
12
13
14
15
16
17
18
19
20
21
22
23
24
25
26
27
28
29
30
31
32
33
34
35
36
37
38
39
40
41
42
43
44
45
46
47
48
49
50
51
52
53
54
55
56
57
58
59
60

- [1] Abou B., Bonn D., Meunier J. , 2001, Phys. Rev. E, **64**, 21510.
- [2] Bellour M., Knaebel A., Harden J.L., Lequeux F., Munch J-P., 2003, Phys. Rev. E, **67**, 31405.
- [3] Bonn D., Tanaka H., Wegdam G., Kellay H., Meunier J., 1998, Europhys. Lett., **45**, 52.
- [4] Gabriel J.C.P., Sanchez C., Davidson P., 1996, J. Phys. Chem., **100**, 11139.
- [5] Knaebel A., Bellour M., Munch J-P., Viasnoff V., Lequeux, F. ; Harden, J.L.; 2000, Europhys. Lett., **52**, 73.
- [6] Kroon K., Wegdam G.H., Sprik S., 1996, Phys.Rev. E, **54**, 6541.
- [7] Kroon M., Vos W.L., Wegdam G.H. , 1998, Phys. Rev. E, **57**, 1962.
- [8] Laponite technical bulletin L204/01 g, Laporte I. Ltd, Cheshire, U.K., pp 1-11.
<http://www.Laponite.com.bulletins.htm>
- [9] Martin C., Pignon F., Piau J.M., Magnin A., Lindner P., Cabane B., 2002, Phys. Rev. E, **66**, 21401.
- [10] Mongondry P., Tassin J.F., Nicolai T. , 2005, J. Colloid Interface Sci., **283**, 397.
- [11] Mourchid A., Lècolier E., Van Damme H., Levitz P., 1998, Langmuir, **14**, 4718.
- [12] Mourchid A., Levitz P., 1998, Phys. Rev. E, **57**, R4887.
- [13] Nicolai T., Cocard S. , 2001, J. Colloid Interface Sci., **244**, 51.
- [14] Nicolai T., Cocard S., 2001, Eur. Phys. J. E, **5**, 221.
- [15] Pignon F., Magnin A., Piau J.M., Cabane B., Lindner P., Diat O., 1997, Phys. Rev. E, **56**, 3281.
- [16] Schosseler F., Kaloun S., Skouri M., Munch J. P., 2006, Phys. Rev. B, **73**, 21401.
- [17] Ruzicka B., Zulian L., Ruocco G. , 2004, Phys. Rev. Lett., **93**, 258301.
- [18] Ruzicka B., Zulian L., Ruocco G. , 2004, J. of Phys. Cond. Matt., **16**, S4993.
- [19] Ruzicka B., Zulian L., Ruocco G. , 2006, Langmuir, **22**, 1106.

1
2
3 [20] Tanaka H., Meunier J., Bonn D., 2004, Phys. Rev. E , **69**, 31404.
4
5

6 [21] Thompson D.W., Butterworth J.T., 1991, J. Colloid Interface Sci., **151**, 236.
7
8
9

10 11 **Figure caption**

12
13 Figure 1.

14
15 Evolution of the photon correlation spectra for two samples at different clay concentrations ($C_w =$
16 2.5 % - panel A and $C_w = 1.0$ % - panel B) for $C_s = 2 \times 10^{-3}$ M at increasing waiting times (reported in
17 the figure) from left to right (as indicated by the arrows). Both samples experience ageing following
18 two different dynamical routes. The final non-ergodic state is signaled by an incomplete decay of
19 the autocorrelation function (uppermost curves). The fitted curves of the ergodic autocorrelation
20 functions are reported as full lines superimposed on the experimental points.
21
22
23
24
25
26
27
28
29
30
31

32
33 Figure 2.

34
35 Values of τ_2 (■) τ_m (○) and τ_{m2} (Δ) as a function of waiting time t_w for two different concentrations,
36 $C_w = 2.5\%$ (top panel) and $C_w = 0.6\%$ (bottom panel) at a salt concentration of $C_s = 1 \times 10^{-3}$ M. The
37 general trend of the three correlation times is essentially the same for both samples. The full lines
38 show the experimental fits of the τ_m data with Eq.(2).
39
40
41
42
43
44
45

46
47 Figure 3.

48
49 Values of the β parameter as a function of τ_m for all the investigated clay and salt concentrations
50 (the amount of NaCl salt is decreasing from panel A to panel D). At a fixed salt concentration all
51 the curves collapse on a single master curve.
52
53
54
55

56
57
58 Figure 4.
59
60

Behaviour of the β parameter as a function of τ_m for different clay and salt concentrations: (8) $C_w = 2.5\%$, $C_s = 1 \times 10^{-4} \text{ M}$; (\square) $C_w = 1.5\%$, $C_s = 1 \times 10^{-3} \text{ M}$; (\circ) $C_w = 1.8\%$, $C_s = 2 \times 10^{-3} \text{ M}$; (X) $C_w = 1.4\%$, $C_s = 5 \times 10^{-3} \text{ M}$. The general trend observed for fixed salt concentration (Fig. 3) can be extended also to samples with different salt concentrations which collapse onto a single master curve.

Figure 5.

Concentration dependence of B (panel A) and t_w^∞ (panel Bkj) parameters for all the investigated clay and salt concentrations (decreasing from top to bottom).

(A) - The transition from a constant value for the “low” concentration samples (\circ) toward another constant value for the “high” concentration samples (\bullet) is an indication of a transition between two different arrested states. The dashed lines reported in the figure are sigmoidal fits of the B parameter.

(B) - The t_w^∞ parameter is decreasing where the clay and/or salt concentrations are increasing. The more concentrated the sample or the bigger is the ionic strength of the solution, the less is the time to reach the final arrested state.

Figure 6.

New phase diagram of Laponite suspensions in water. All the investigated samples are reported as low (\circ) and high (\bullet) concentrations. The stars are the results of the sigmoidal fits of the B parameter reported in Fig. 5. The solid-dashed line is an eye indication for the hypothesized transition line between the two regions of arrested states, IG1 and IG2, discussed in the paper.

1
2
3
4
5
6
7
8
9
10
11
12
13
14
15
16
17
18
19
20
21
22
23
24
25
26
27
28
29
30
31
32
33
34
35
36
37
38
39
40
41
42
43
44
45
46
47
48
49
50
51
52
53
54
55
56
57
58
59
60

For Peer Review Only

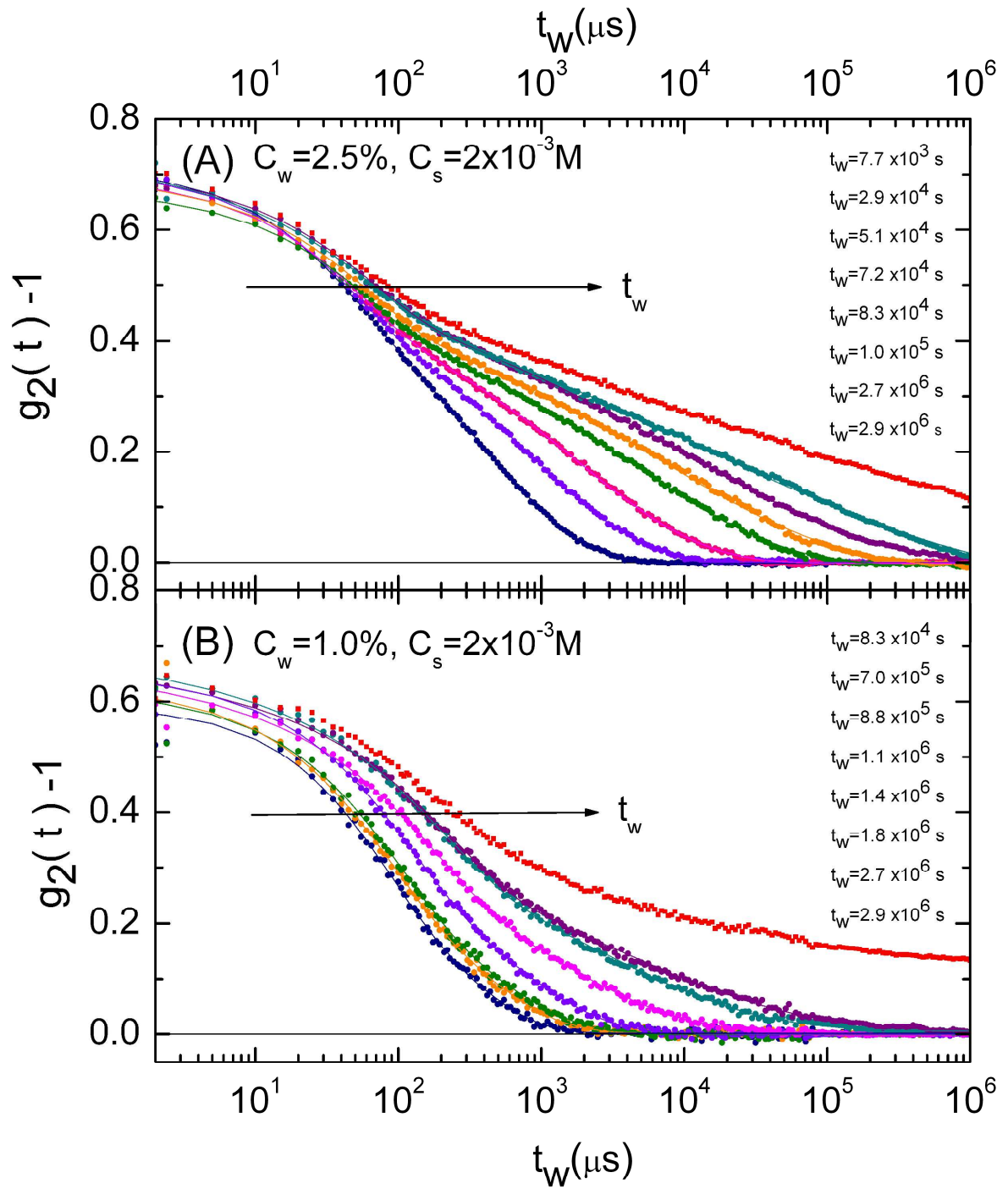


FIGURE 1

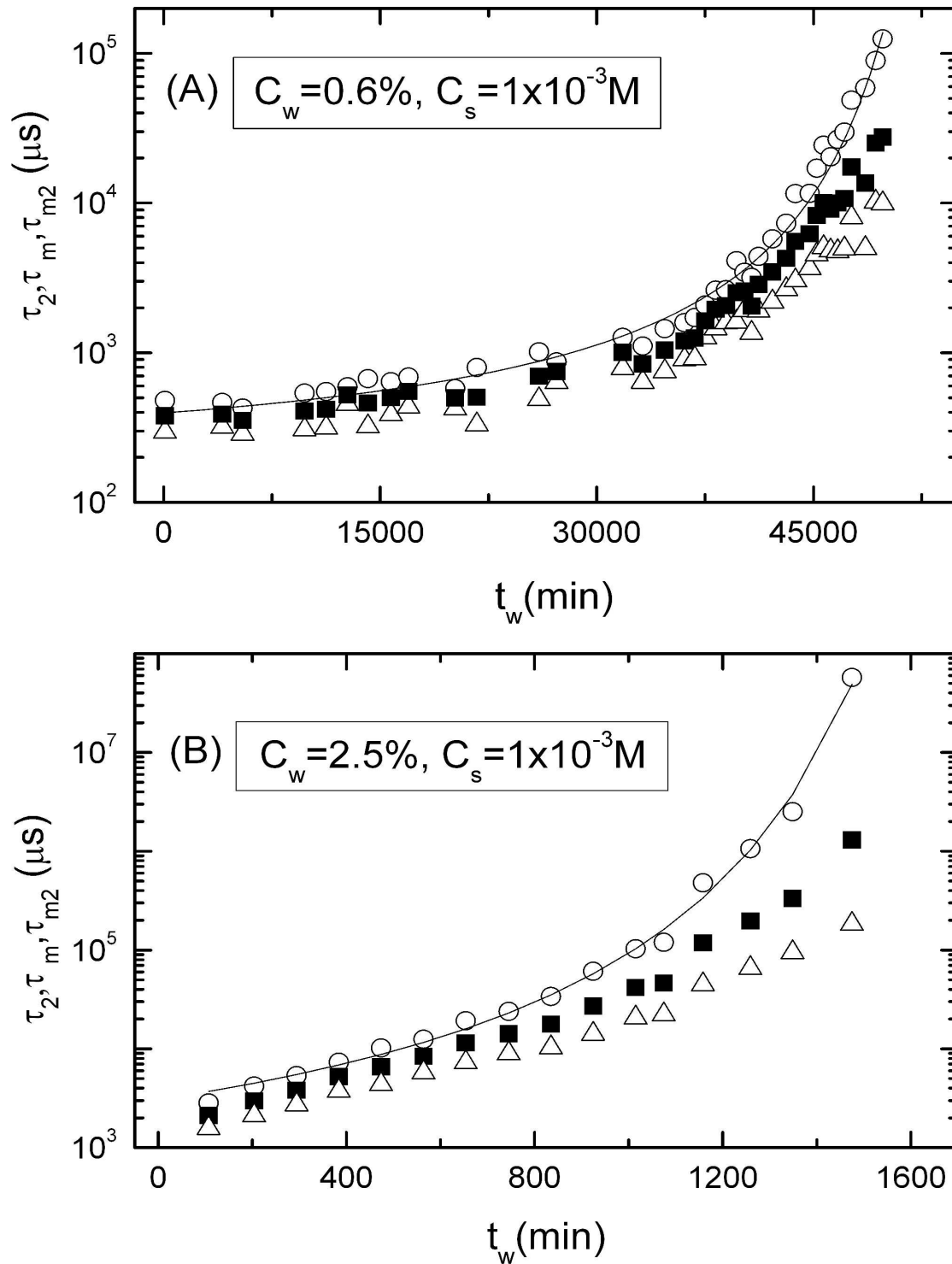


FIGURE 2

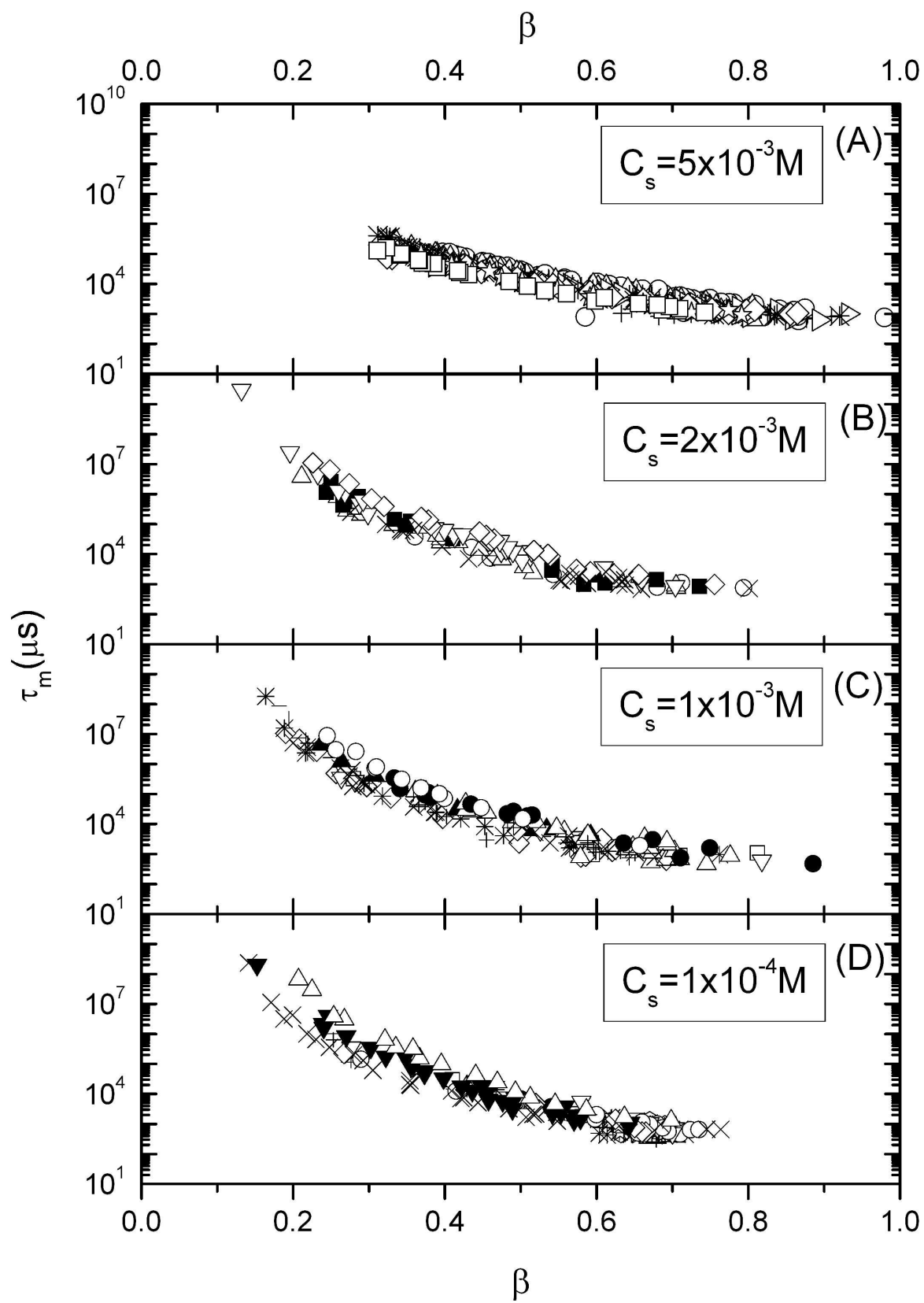


FIGURE 3

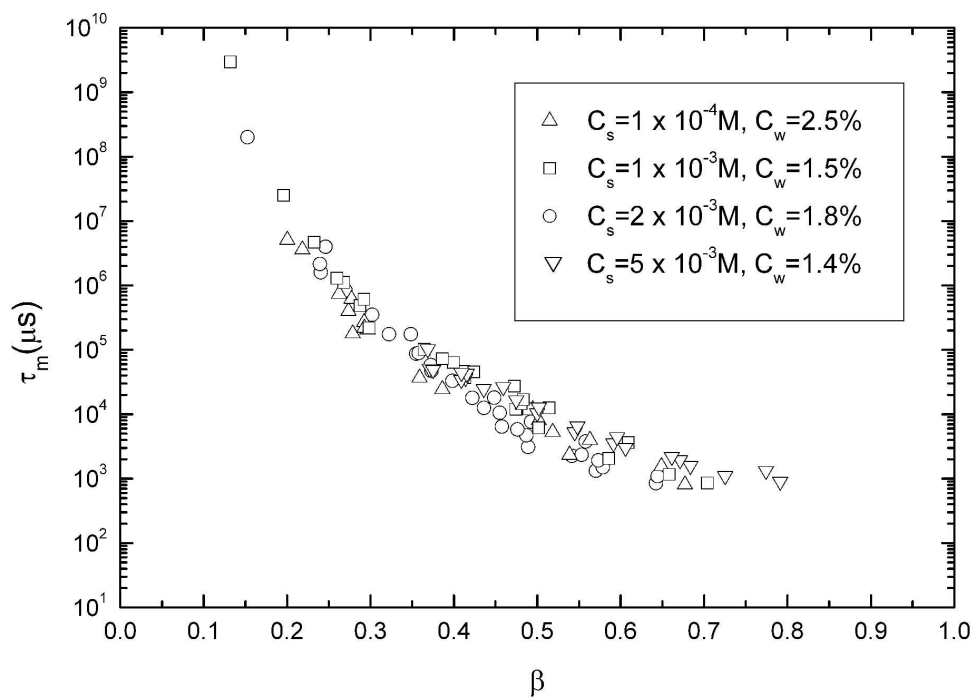


FIGURE 4

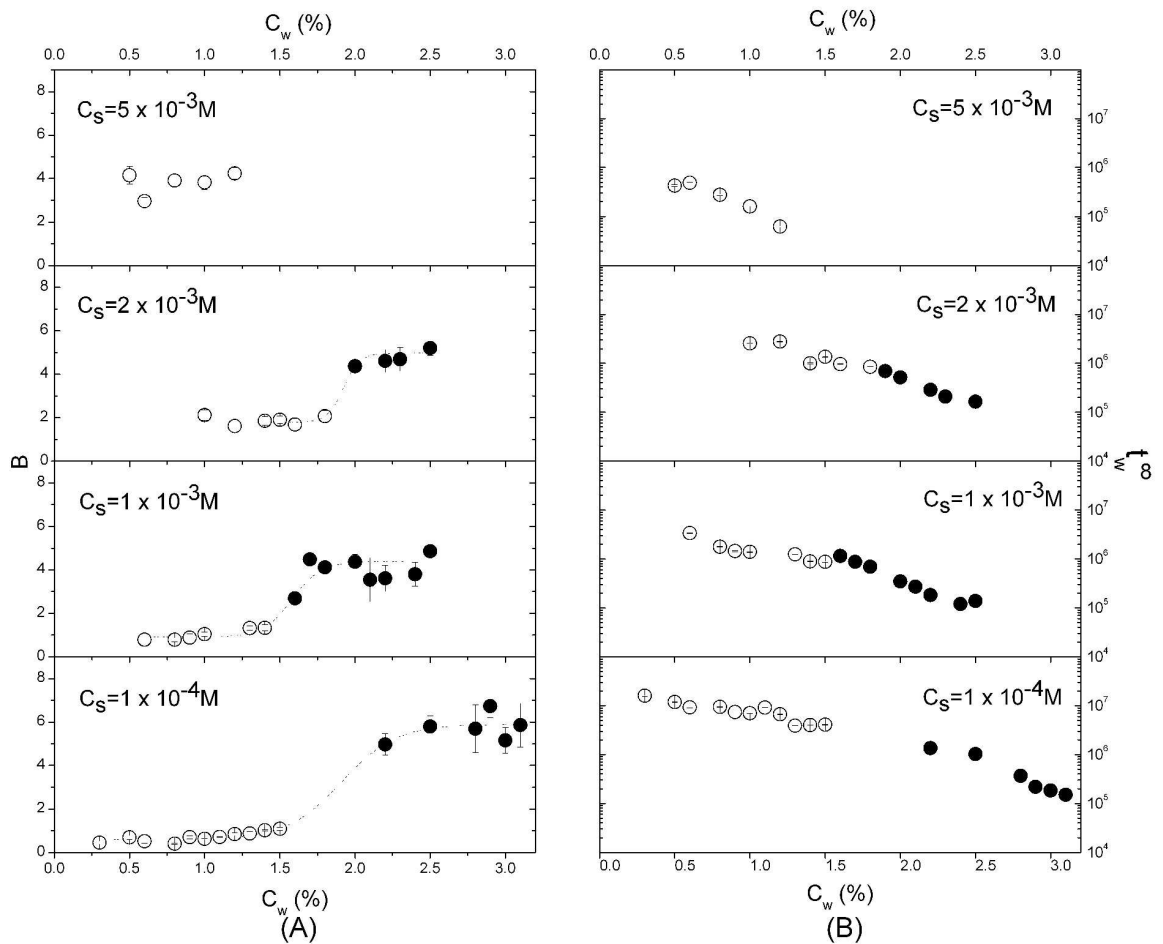


FIGURE 5

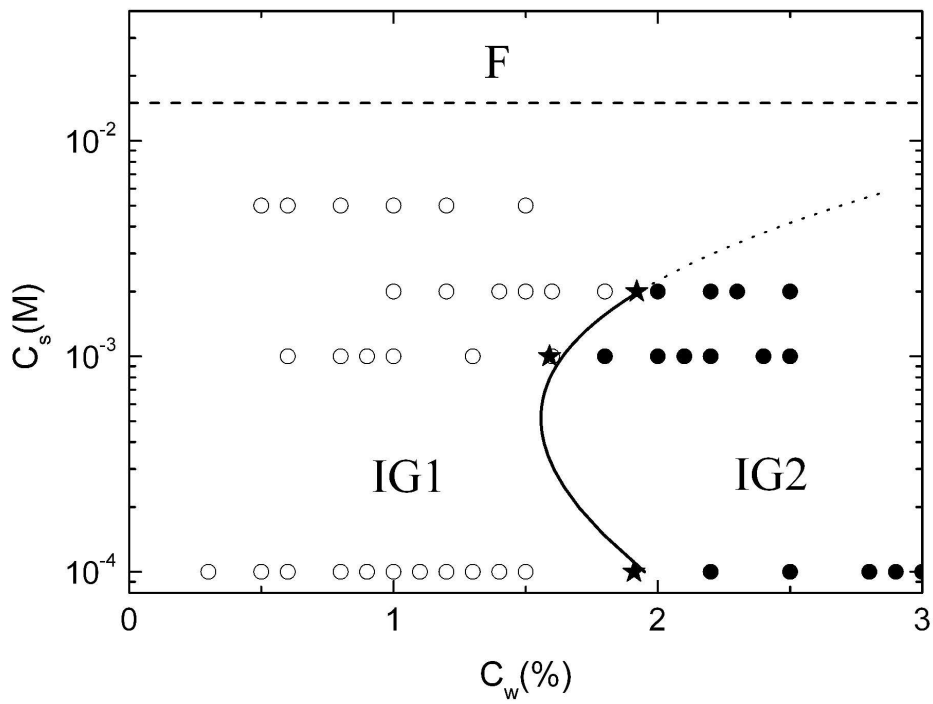


FIGURE 6